Dynamics of the Reaction of Hydrogen Peroxide with a Water Soluble Non μ-Oxo Dimer Forming Iron(III) Tetraphenylporphyrin. 2. The Reaction of Hydrogen Peroxide with 5,10,15,20-Tetrakis(2,6-dichloro-3-sulfonatophenyl)-porphinatoiron(III) in Aqueous Solution

Rick Panicucci and Thomas C. Bruice*

Contribution from the Department of Chemistry, University of California at Santa Barbara, Santa Barbara, California 93106. *Received December 15, 1989*

Abstract: The reaction of hydrogen peroxide with 5,10,15,20-tetrakis(2,6-dichloro-3-sulfonatophenyl)porphinatoiron(III) hydrate [(**2**)$Fe^{III}(H_2O)(X)$, where X = H_2O or HO^-, dependent on pH] has been studied in water between pH 0.5 and 12.25 and in D_2O between pD 3.3 and 10.70 (30 °C, μ = 0.2 with $NaNO_3$) by using 2,2'-azinobis(3-ethylbenzthiazoline)sulfonate (ABTS) as a trap for oxidizing intermediates. The reaction is first-order in both (**2**)$Fe^{III}(H_2O)(X)$ and hydrogen peroxide and zero-order in ABTS. The pH (pD) dependence of the log of the second-order rate constant (k_{ly}) exhibits three plateau regions showing that there are three reaction paths. Transition-state compositions are at low pH, (**2**)$Fe^{III}(H_2O)(H_2O_2)$; around neutrality, (**2**)$Fe^{III}(HO^-)(H_2O_2)$; and at high pH, (**2**)$Fe^{III}(HO^-)(HO_2^-)$. Comparison of the pH dependence of log k_{ly}^H in H_2O to the pD dependence of log k_{ly}^D in D_2O allows the determination of the deuterium solvent kinetic isotope effect for the decomposition of (**2**)$Fe^{III}(H_2O)(H_2O_2)$/(**2**)$Fe^{III}(D_2O)(D_2O_2)$ (k_1^H/k_1^D = 3) and (**2**)$Fe^{III}(HO^-)(H_2O_2)$/(**2**)$Fe^{III}(DO^-)(D_2O_2)$ (k_2^H/k_2^D = 1.2). A solvent kinetic isotope effect of 3 is in accord with H-O bond breaking accompanying O-O bond breaking (general-base catalysis by lyate species), while an isotope effect of 1.2 is to be anticipated as a solvent effect accompanying transfer from H_2O to D_2O. Carboxylic acid/carboxylate and other oxygen acid/oxygen base buffers do not serve as general catalysts at any pH. In contrast the sterically hindered nitrogen bases 2,6-dimethylpyridine, 2,4,6-trimethylpyridine, and 4-methoxy-2,6-dimethylpyridine act as general-base catalysts for the decomposition of the critical species formed at low pH (i.e, (**2**)-$Fe^{III}(H_2O)(H_2O_2)$). By using 2,4,6-trimethylpyridine/2,4,6-trimethylpyridine·H(D)$^+$ buffers in H_2O and D_2O, the deuterium solvent isotope effect for nitrogen base catalysis was determined as 3.3. Thus, H_2O and nitrogen bases act as general base catalysts at low pH with isotope effects around 3. The Bronsted constant β was determined to be ~0.1 for the nitrogen bases (B:). Various mechanisms are considered. Previous studies have shown that an iron(IV)-oxo porphyrin does not epoxidize 3-cyclohexene-1-carboxylic acid. In this study we show that (**2**)$Fe^{III}(H_2O)_2$ does not catalyze the epoxidation of 3-cyclohexene-1-carboxylic acid (1.0 M) by H_2O_2 (0.1 M) in water at pH 7.0. Lack of general catalysis in the decomposition of the peroxide ligated species at intermediate pH ((**2**)$Fe^{III}(HO^-)(H_2O_2)$) requires explanation based upon the distal ligand being HO^- rather than H_2O. We propose that the more basic HO^- ligand increases the electron density on iron allowing $1e^-$ transfer to ligated H_2O_2 without proton removal. The pK_a of (**2**)$Fe^{III}(H_2O)_2 \rightarrow$ (**2**)$Fe^{III}(HO^-)(H_2O) + H^+$ has been determined as 7.85 (8.68 in D_2O). Comparison of this to the pK_a (7.25) for proton dissociation from 5,10,15,20-tetrakis(2,6-dimethyl-3-sulfonatophenyl)porphinatoiron(III) hydrate (i.e., (**1**)$Fe^{III}(H_2O)_2$) shows that the field effect of eight methyl groups surrounding the ligated water molecules is acid strengthening compared to eight chloro substituents.

Introduction

Studies of the protoporphyrin-IX containing peroxidases, catalases, and, in particular, cytochrome P-450 enzymes have drawn the interest of numerous chemists with the resultant emergence of a chemistry subdiscipline. Our interests have, in the main, revolved around two chemical problems: (a) the mechanisms by which porphinato-metal salts undergo $1e^-$ and $2e^-$ oxidation with accompanying oxygen transfer to the metal moiety[1] and (b) the mechanism of epoxidation of alkenes by higher valent metallo-oxo porphinato species.[2] The first appropriately designed study of the reaction of an oxidative oxygen transfer agent with a porphinato-metal salt in aqueous solution involved hydrogen peroxide as oxygen donor and 5,10,15,20-tetrakis(2,6-dimethyl-3-sulfonatophenyl)porphinatoiron(III) hydrate ((**1**)$Fe^{III}(H_2O)_2$).[1n] The design of (**1**)$Fe^{III}(H_2O)_2$ prevents μ-oxo dimer formation and aggregation so that in dynamic studies one need not be concerned with other than monomeric species. In order to determine the rate constants we introduced the water soluble 2,2'-azinobis(3-ethylbenzthiazoline)sulfonate (ABTS) as a trap for (**1**)$Fe^{IV}(O)(X)$ and (**1**$^{\bullet+}$)$Fe^{IV}(O)(X)$ intermediate species formed in the rate-determining step. The advantage of ABTS, which is employed in clinical medicine, is an independence of its $1e^-$ redox potential on pH. One-electron oxidation of ABTS gives the $ABTS^{\bullet+}$ (660 nm).

We now report the results of a study of the reaction of hydrogen peroxide with 5,10,15,20-tetrakis(2,6-dichloro-3-sulfonatophenyl)porphinatoiron(III) hydrate, (**2**)$Fe^{III}(H_2O)_2$. Substitution of the eight ortho-methyl groups of (**1**)$Fe^{III}(H_2O)_2$ with eight

(1) (a) Balasubramanian, P. N.; Lee, R. W.; Bruice, T. C. *J. Am. Chem. Soc.* **1989**, *111*, 8714. (b) Balasubramanian, P. N.; Lindsay Smith, J. R.; Davies, M. J.; Kaaret, T. W.; Bruice, T. C. *J. Am. Chem. Soc.* **1989**, *111*, 1477. (c) Bruice, T. C.; Balasubramanian, P. N.; Lee, R. W.; Lindsay Smith, J. R. *J. Am. Chem. Soc.* **1988**, *110*, 7890. (d) Lindsay Smith, J. R.; Balasubramanian, P. N.; Bruice, T. C. *J. Am. Chem. Soc.* **1988**, *110*, 7411. (e) Lee, W. A.; Lung-Chi, Y.; Bruice, T. C. *J. Am. Chem. Soc.* **1988**, *110*, 4277. (f) Dicken, C. M.; Balasubramanian, P. N.; Bruice, T. C. *Inorg. Chem.* **1988**, *27*, 197. (g) Balasubramanian, P. N.; Schmidt, E. S.; Bruice, T. C. *J. Am. Chem. Soc.* **1987**, *109*, 7865. (h) Ostovic, D.; Knobler, C. B.; Bruice, T. C. *J. Am. Chem. Soc.* **1987**, *109*, 3444. (i) Bruice, T. C.; Dicken, C. M.; Balasubramanian, P. N.; Woon, T. C.; Lu, F. L. *J. Am. Chem. Soc.* **1987**, *109*, 3436. (j) Wong, Wah-Hum; Ostovic, D.; Bruice, T. C. *J. Am. Chem. Soc.* **1987**, *109*, 3428. (k) Woon, T. C.; Dicken, C. M.; Bruice, T. C. *J. Am. Chem. Soc.* **1986**, *108*, 7990. (l) Calderwood, T. S.; Bruice, T. C. *Inorg. Chem.* **1986**, *25*, 3722. (m) Schmidt, E. S.; Bruice, T. C.; Brown, R. S.; Wilkins, C. L. *Inorg. Chem.* **1986**, *25*, 4799. (n) Zipplies, M. F.; Lee, W. A.; Bruice, T. C. *J. Am. Chem. Soc.* **1986**, *108*, 4433. (o) Lung-Chi, Y.; Bruice, T. C. *J. Am. Chem. Soc.* **1986**, *108*, 1643. (p) Dicken, C. M.; Woon, T. C.; Bruice, T. C. *J. Am. Chem. Soc.* **1986**, *108*, 1636. (q) Lee, W. A.; Bruice, T. C. *Inorg. Chem.* **1986**, *25*, 131. (r) Lung-Chi, Y.; Calderwood, T. S.; Bruice, T. C. *J. Am. Chem. Soc.* **1985**, *107*, 8273. (s) Calderwood, T. S.; Lee, W. A.; Bruice, T. C. *J. Am. Chem. Soc.* **1985**, *107*, 8272. (t) Dicken, C. M.; Lu, F. L.; Nee, M. W.; Bruice, T. C. *J. Am. Chem. Soc.* **1985**, *107*, 5776. (u) Lee, W. A.; Calderwood, T. S.; Bruice, T. C. *Proc. Natl. Acad. Sci. U.S.A.* **1985**, *82*, 4301. (v) Lung-Chi, Y.; Bruice, T. C. *Inorg. Chem.* **1985**, *24*, 986. (w) Lee, W. A.; Bruice, T. C. *J. Am. Chem. Soc.* **1985**, *107*, 513. (x) Lung-Chi, Y.; Bruice, T. C. *J. Am. Chem. Soc.* **1985**, *107*, 512.

0002-7863/90/1512-6063$02.50/0

ortho-chloro substituents to obtain (2)$Fe^{III}(H_2O)_2$ allows an assessment of the influence of electronic effects. The importance of general catalysis, values of deuterium kinetic solvent isotope effects, and approximate Bronsted coefficients have been employed in the formulation of mechanisms.

Experimental Section

Materials. Deionized, double-glass distilled water was used for all experiments. All chemicals were of the best available purity. The 2,2′-azinobis(3-ethylbenzthiazoline)sulfonic acid diammonium salt (ABTS) from Sigma was converted to the disodium salt prior to its use. This was accomplished by adding a dilute solution of the ABTS diammonium salt (0.1 M) to a 1 M $NaNO_3$ solution and collecting the ABTS disodium salt precipitate which was dried in vacuo over P_2O_5. The concentration of hydrogen peroxide (Fisher, 30%) was determined by iodometric analyses prior to use, as described elsewhere.[3] Buffers were prepared by mixing appropriate amounts of the acid and base species and were made free from heavy metal impurities as described previously.[1n] 2,6-Dimethylpyridine (Aldrich) and 2,4,6-trimethylpyridine (Aldrich) were purified according to literature procedures.[4] 4-Methoxy-2,6-dimethylpyridine was prepared by using literature procedures.[5] The pyridines were converted to their HCl salts by bubbling an ethereal solution of the pyridine with dry HCl gas. The pyridine·HCl salts were then recrystallized from methanol/diethyl ether. The pK_a values of 2,6-dimethylpyridine·H^+, 2,4,6-trimethylpyridine·H^+, and 4-methoxy-2,6-dimethylpyridine·H^+ were determined (μ = 0.20, 30 °C) by the method of half-neutralization and were found to be 6.85, 7.47 and 8.09, respectively. The pK_a of 2,4,6-trimethylpyridine·D^+ in D_2O was found to be 8.07.

Instrumentation employed has been described previously.[1n]

Kinetic studies of the reaction of hydrogen peroxide with (2)Fe^{III}-$(H_2O)(X)$ were determined by following the increase of absorbance of $ABTS^{\cdot+}$ at 660 nm at 30 °C as previously described.[1n] The kinetic runs in D_2O (99.8%, Aldrich) were carried out under the same conditions described above for H_2O. Stock solutions of reagents in D_2O were prepared by first exchanging exchangeable protium with D_2O. The value of pD was obtained by adding 0.38[6] to the observed pH of solutions in D_2O.

Porphyrin Synthesis. 5,10,15,20-Tetrakis(2,6-dichlorophenyl)-porphyrin was prepared by condensing 2,6-dichlorobenzaldehyde (Aldrich) and pyrrole (Aldrich) according to the method described by Lindsey et al.[7] Sulfonation of 5,10,15,20-Tetrakis(2,6-dichlorophenyl)porphyrin was carried out following the method described by Dolphin et al.[8] to give 5,10,15,20-tetrakis(2,6-dichloro-3-sulfonatophenyl)porphyrin ((2)H_2). Insertion of iron into (2)H_2 was accomplished by following the method of Zipplies et al.[1n] to give iron(III) 5,10,15,20-tetrakis(2,6-dichloro-3-sulfonatophenyl)porphyrin. Anal. Calcd for $C_{44}H_{16}Cl_8N_4O_{12}S_4FeNa_4 \times 0.5SO_4^{2-} \times 25H_2O \times Na_2SO_4$ (fw 1992.76): C, 26.52; H, 3.33; N, 2.81; S, 8.85; Cl, 14.23; Fe, 2.8; Na, 6.92. Found: C, 26.31; H, 2.94; N, 2.66; S, 9.27; Cl, 13.22; Fe, 2.21; Na, 6.64. R_f (KC_{18}, 2-propanol/water [2% tetrabutylammonium bromide]/methanol = 5:3:2) 0.75, 0.6 (most abundant), and 0.45. The UV/vis spectra at pH 2.8 and 9.8 are shown in Figure 1. The presence of a double Soret band at the low pH may be attributed to a difference in the electronic absorption spectra of atropisomers or to the presence of some partially para-sulfonated isomer.

Results

The water soluble 5,10,15,20-tetrakis(2,6-dichloro-3-sulfonatophenyl)porphyrin ((2)H_2) (in methanol, 423 nm (Soret), 521, 555, 602, and 657 nm) when subjected to reversed-phase thin-layer chromatography revealed three spots. Since the $-SO_3H$ substituents of the four phenyl rings are located at meta positions, there are four possible atropisomers. Reversed-phase thin-layer chromatography shows that two of the atropisomers are much less abundant than the other(s). Metalation of (2)H_2 provided (2)-$Fe^{III}(H_2O)_2$.

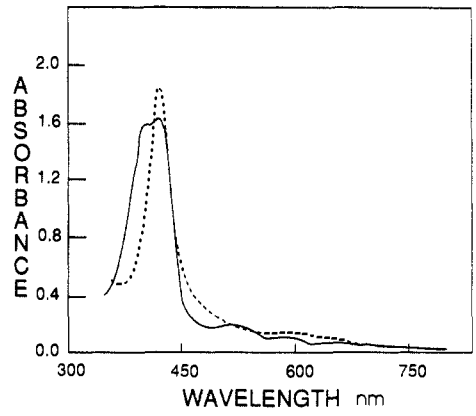

Figure 1. Absorption spectra of (2)$Fe^{III}(H_2O)_2$ at pH 2.8 (—) (0.5 M chloroacetic acid buffer) and (2)$Fe^{III}(H_2O)(OH)$ at pH 9.8 (- · -) (0.5 M carbonate buffer). The molar absorptivities were found to be 9.2 × 10^4 and 1 × 10^5 M^{-1} cm^{-1} for (2)$Fe^{III}(H_2O)_2$ and (2)$Fe^{III}(H_2O)(OH)$, respectively.

The pK_a Values of (2)$Fe^{III}(Y_2O)_2$ (Y = H or D) Species Were Determined by Spectrophotometric Titration in H_2O and D_2O, Respectively (30 °C, μ = 0.2 with $NaNO_3$). The iron(III) porphyrin salt exhibits identical visible absorption spectrum in H_2O and D_2O. Spectrophotometric titration was carried out between

$$(2)Fe^{III}(Y_2O)_2 \rightleftharpoons (2)Fe^{III}(Y_2O)(YO^-) + Y^+ \qquad (1)$$

Y = H or D

pH(D) 2 and 14. The least-squares pK_a's of 7.85 ± 0.1 for water and 8.68 ± 0.15 for D_2O were determined by the fitting of the changes in absorbance (at both 401 and 423 nm) with pH(D) to a theoretical curve for the dissociation of a monoprotic acid. This observation clearly demonstrates that all the atropisomers of (2)$Fe^{III}(Y_2O)_2$ possess indistinguishable pK_a values. Thus, the electronic nature of the Fe^{III} of the atropisomers are the same. Evidence of a second deprotonation step could not be observed spectrophotometrically.

Kinetics of the Reaction of (2)$Fe^{III}(H_2O)(X)$ with Hydrogen Peroxide. The reaction of (2)$Fe^{III}(H_2O)(X)$ (X = H_2O or $-OH$) with hydrogen peroxide was examined between pH 0.5 and 12.25 (30 °C; μ = 0.2 with $NaNO_3$) with ABTS as a trap for higher valent iron-oxo porphyrin intermediates. One-electron oxidation of ABTS → $ABTS^{\cdot+}$ was followed at 660 nm (ϵ = 12000 M^{-1} cm^{-1}). In the absence of (2)$Fe^{III}(H_2O)(X)$, hydrogen peroxide and ABTS do not react to provide $ABTS^{\cdot+}$. Reactions were carried out under the pseudo-first-order conditions of [(2)Fe^{III}-$(H_2O)(X)$] < [H_2O_2] ≪ [ABTS]. The appearance of $ABTS^{\cdot+}$ (ΔA_{660}) vs time was fit to the first-order rate law to obtain pseudo-first-order rate constants (k_{obsd}).

The Dependence of k_{obsd} on the Concentrations of Trapping Agent and Reactants. Values of k_{obsd} were determined over a 10-fold change in concentration of (2)$Fe^{III}(H_2O)(X)$ (5 × 10^{-7}-5 × 10^{-6}) at constant pH, $[H_2O_2]_i$ of 5 × 10^{-5} M, and $[ABTS]_i$ of 7 × 10^{-3} M. Throughout the pH range investigated, k_{obsd} increased linearly as a function of [(2)$Fe^{III}(H_2O)(X)$] at a given pH value. A sampling of the data is shown in Figure 2. Thus, the reaction of H_2O_2 with (2)$Fe^{III}(H_2O)(X)$ is first-order in the latter.

The order in [ABTS] was determined at pH 6.70 (0.05 M phosphate, 30 °C and μ = 0.2) with [(2)$Fe^{III}(H_2O)(X)$] and [H_2O_2] constant at 1 × 10^{-6} and 5 × 10^{-5} M, respectively. The concentration of ABTS was varied 10-fold (1 × 10^{-3}–1 × 10^{-2} M). Values of k_{obsd} were constant (2.46 × 10^{-4}–2.68 × 10^{-4} s^{-1}) showing the appearance of $ABTS^{\cdot+}$ to be zero-order in ABTS.

(2) (a) Ostovic, D.; Bruice, T. C. *J. Am. Chem. Soc.* **1989**, *111*, 6511. (b) Garrison, J. M.; Ostovic, D.; Bruice, T. C. *J. Am. Chem. Soc.* **1989**, *111*, 4960. (c) Lee, R. W.; Nakagaki, P. C.; Bruice, T. C. *J. Am. Chem. Soc.* **1989**, *111*, 1368. (d) Garrison, J. M.; Bruice, T. C. *J. Am. Chem. Soc.* **1989**, *111*, 191. (e) Castellino, A. J.; Bruice, T. C. *J. Am. Chem. Soc.* **1988**, *110*, 7512. (f) Ostovic, D.; Bruice, T. C. *J. Am. Chem. Soc.* **1988**, *110*, 6906. (g) Castellino, A. J.; Bruice, T. C. *J. Am. Chem. Soc.* **1988**, *110*, 1313. (h) Lee, R. W.; Nakagaki, P. C.; Balasubramanian, P. N.; Bruice, T. C. *Proc. Natl. Acad. Sci. U.S.A.* **1988**, *85*, 641. (i) Castellino, A. J.; Bruice, T. C. *J. Am. Chem. Soc.* **1988**, *110*, 158. (j) Balasubramanian, P. N.; Sinha, A.; Bruice, T. C. *J. Am. Chem. Soc.* **1987**, *109*, 1456.

(3) Bruice, T. C.; Noar, J. B.; Ball, S. S.; Venkataram, U. V. *J. Am. Chem. Soc.* **1983**, *105*, 2452.

(4) Perrin, D. D.; Armarego, W. L. F. *Purification of Laboratory Chemicals*, 3rd ed.; Pergamon Press: Oxford, 1988.

(5) Bojarska-Dahlig, H. N. *Recl. Trav. Chim. Pays-Bas* **1958**, *77*, 331.

(6) Fife, T. H.; Bruice, T. C. *J. Phys. Chem.* **1961**, *65*, 1079.

(7) Lindsey, J. S.; Wagner, R. W. *J. Org. Chem.* **1989**, *54*, 828.

(8) Dolphin, D.; Nakano, T.; Maione, T. E.; Kirk, T. K.; Farrell, R. *Synthetic Model Ligninases, in Lignin Enzymic and Microbial Degradation*; Odier, E., Ed.; INRA Publications: Paris, 1987; p 157.

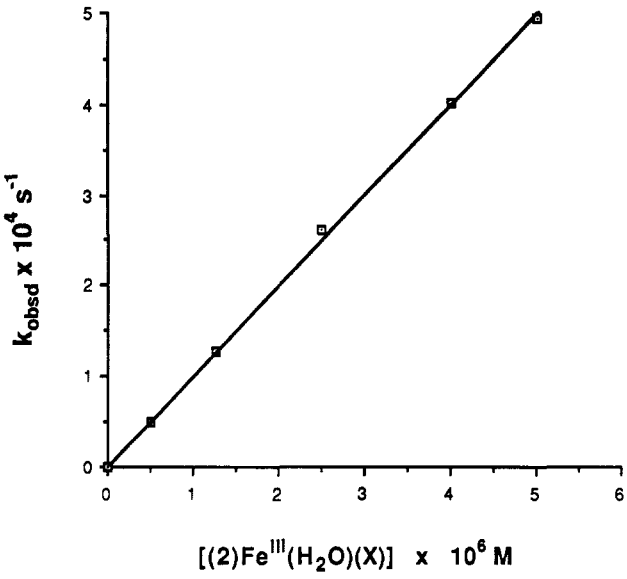

Figure 2. Observed first-order rate constants at pH 4.7 (0.05 M acetate buffer 30 °C and μ = 0.2) for the formation of $ABTS^{\bullet+}$ as a function of [(2)$Fe^{III}(H_2O)(X)$]. The initial concentrations of H_2O_2 and ABTS were 5 × 10^{-5} and 7 × 10^{-3} M, respectively.

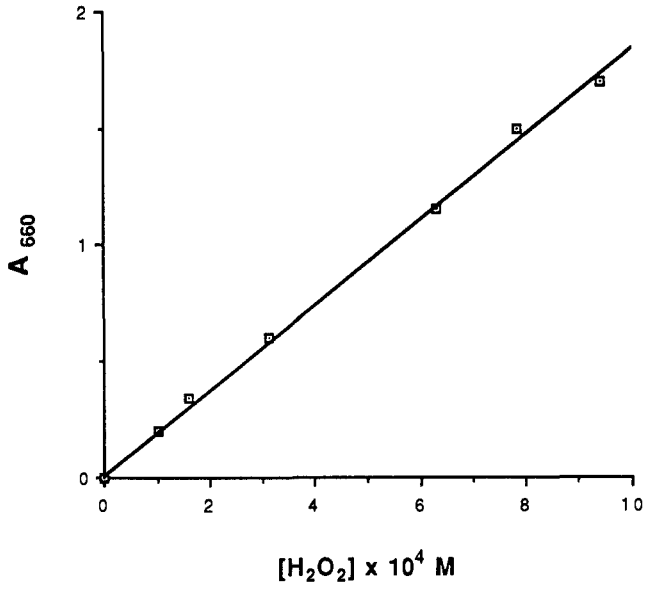

Figure 3. Final absorbance at 660 nm (A_{660}) as a function of $[H_2O_2]_i$ (9.4 × 10^{-6}–9.4 × 10^{-5} M). [(2)$Fe^{III}(H_2O)(X)$] = 1 × 10^{-6} M, [ABTS] = 7 × 10^{-3} M, pH 6.70 (0.05 M phosphate buffer, μ = 0.2) at 30 °C.

Dependence of k_{obsd} upon the concentration of H_2O_2 (pH 6.70) was determined from experiments by using a 10-fold range of $[H_2O_2]$ (9.4 × 10^{-6}–9.4 × 10^{-5} M) while holding [(2)$Fe^{III}(H_2O)(X)$] and [ABTS] constant at 1 × 10^{-6} and 7 × 10^{-3} M, respectively. The value of k_{obsd} was found to be constant (2.56 × 10^{-4}–2.60 × 10^{-4} s^{-1}). This result is as expected of a process which involves the catalytic conversion of an oxidant to products under pseudo-first-order conditions of [oxidant] ≫ [catalyst] (eq 2). A plot of the final absorbance at 660 nm vs $[H_2O_2]_i$ reveals

$$(2)Fe^{III}(YOH)(X) + 2H_2O_2 \rightarrow (2)Fe^{III}(YOH)(X) + 2H_2O + O_2 \quad (2a)$$

$$(2)Fe^{III}(YOH)(X) + H_2O_2 + 2ABTS + 2H^+ \rightarrow (2)Fe^{III}(YOH)(X) + 2H_2O + 2ABTS^{\bullet+} \quad (2b)$$

a linear dependence of the yield of $ABTS^{\bullet+}$ upon H_2O_2 concentration (Figure 3). The yield of $ABTS^{\bullet+}$ is dependent on $[ABTS]_i$ (data not shown). This is consistent[1n] with a competition between H_2O_2 (eq 2a) and ABTS (eq 2b) for intermediate higher valent iron-oxo porphyrin formed in the rate-determining step. The slope of a plot of $ABTS^{\bullet+}$ absorbance vs $[H_2O_2]_i$ represents the fraction of capture of intermediate higher valent iron-oxo porphyrin by ABTS. From the data of Figure 3, at pH = 6.70, 75% of higher valent iron-oxo porphyrin is captured by ABTS, and the remaining 25% is captured by H_2O_2.[1n] This is consistent with the finding that in the absence of ABTS, O_2 is produced in 100% yield based upon $[H_2O_2]_i$. The yield of $ABTS^{\bullet+}$ varies with pH (100% at pH < 2, decreasing as pH increases to <20% at pH 12.25) due to the trapping efficiencies for the higher valent iron-oxo porphyrin being HO_2^- > ABTS > H_2O_2. (We have shown that hydrogen peroxide and ABTS rapidly reduce both iron(IV)-oxo porphyrin and iron(IV)-oxo porphyrin π-cation radical to iron(III) porphyrin.[1a,b,c])

Table I. Values of the Second-Order Rate Constant (k_2'), for the Reaction of (2)$Fe^{III}(H_2O)(X)$ with H_2O_2, at Various pH Values at Two [B_T] Values (30 °C, μ = 0.2)

pH	buffer	[B_T], mM	k_2, M^{-1} s^{-1}
2.80	chloroacetate	50	60
2.80	chloroacetate	5	55
4.70	acetate	50	90
4.70	acetate	5	85
6.70	phosphate	50	256
6.70	phosphate	5	263
6.85	2,6-dimethylpyridine	50	1060
6.85	2,6-dimethylpyridine	5	460
7.47	2,4.6-trimethylpyridine	50	1700
7.47	2,4.6-trimethylpyridine	5	883
8.09	4-methoxy-2,6-dimethylpyridine	50	2640
8.09	4-methoxy-2,6-dimethylpyridine	5	1230
9.15	carbonate	50	1700
9.15	carbonate	5	1500

These experiments establish that the reaction of interest is first-order in both [(2)$Fe^{III}(H_2O)(X)$] and $[H_2O_2]$ and zero-order in [ABTS]. The oxidation of (2)$Fe^{III}(H_2O)(X)$ by H_2O_2 to form intermediate higher valent iron-oxo porphyrin is rate-limiting so that $ABTS^{\bullet+}$ formation (eq 2b) follows eq 3.

$$d[ABTS^{\bullet+}]/dt = k_2'[(2)Fe^{III}(H_2O)(X)][H_2O_2] \quad (3)$$

$$\text{where } k_{obsd} = k_2'[(2)Fe^{III}(H_2O)(X)]$$

Effect of Buffers on the Rate of Reaction of (2)$Fe^{III}(H_2O)(X)$ with Hydrogen Peroxide. The rate constant for buffer catalysis at a constant pH is defined as k_{BT} and the rate constant for the buffer independent rate at constant pH as k_{ly}. When buffer catalysis is involved, the apparent second-order rate constant (of eq 3) $k_2' = (k_{ly} + k_{BT}[B_T])$, where [total buffer] = $[B_T]$ = [B:] + $[BH^+]$. The effects of buffers on k_2' were obtained by determining k_{obsd} at constant values of pH and constant initial concentrations of (2)$Fe^{III}(H_2O)(X)$ and H_2O_2 and varying [B_T] (5–50 mM). The following buffers were used: $ClCH_2COOH/ClCH_2COO^-$ (pH 2.8), CH_3COOH/CH_3COO^- (pH 4.0, 4.7, and 5.5), $H_2PO_4^-/HPO_4^{2-}$ (pH 6.70 and 7.70), 2,6-dimethylpyridine·H^+/2,6-dimethylpyridine (pH 5.85, 6.85, and 7.85), 2,4,6-trimethylpyridine·H^+/2,4,6-trimethylpyridine (pH 6.47, 6.85, 7.00, 7.47, and 8.47), 4-methoxy-2,6-dimethylpyridine·H^+/4-methoxy-2,6-dimethylpyridine (pH 7.10, 8.09, and 9.10), and HCO_3^-/CO_3^{2-} (pH 9.15 and 9.85). The apparent second-order rate constant (k_2') in the presence of the various buffers at 5 and 50 mM ([B_T]) are given in Table I. It is evident that the value of k_2' is insensitive to a 10-fold change in [B_T] for the (oxy acid)/(oxy anion) buffers. In a single experiment the concentration of CH_3COOH/CH_3COO^- (pH 4.0) was varied between 0.04 and 0.4 M. Again, buffer catalysis was not observed. However, a catalytic effect is observed with all the nitrogen buffers (2,6-dimethylpyridine, 2,4,6-trimethylpyridine, and 4-methoxy-2,6-dimethylpyridine). The observations with all the nitrogen buffers were similar, and we have chosen the results obtained with 2,4,6-trimethylpyridine for illustration. A sampling of the plots of k_{obsd} vs [(2)$Fe^{III}(H_2O)(X)$] at different 2,4,6-trimethylpyridine concentrations at constant pH (7.00) is provided in Figure 4. Inspection of Figure 4 shows that k_2' (slopes) increases with increasing [B_T]. The values of k_2' when plotted vs [B_T] (Figure 5) provide k_{BT} as slope and k_{ly} as the intercept. The pH dependent

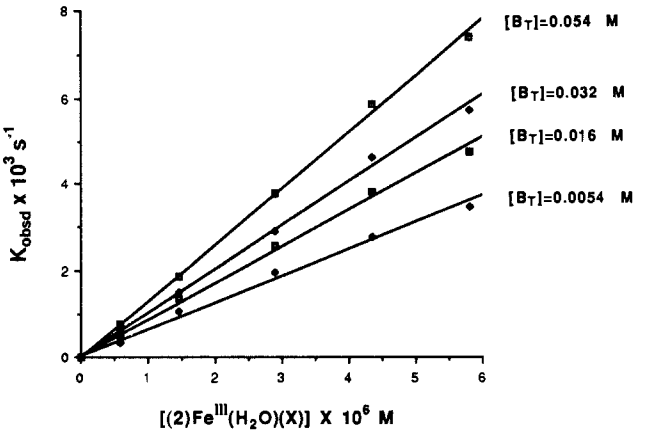

Figure 4. Dependence of the pseudo-first-order rate constants (k_{obsd}) on the concentration of 2,4,6-trimethylpyridine buffer at pH 7.00 (30 °C, μ = 0.2). With initial concentrations of [(**2**)$Fe^{III}(H_2O)(X)$] = 5.0 × 10^{-7}–5.0 × 10^{-6} M, [H_2O_2] = 5 × 10^{-5} M, and [ABTS] = 7 × 10^{-3} M.

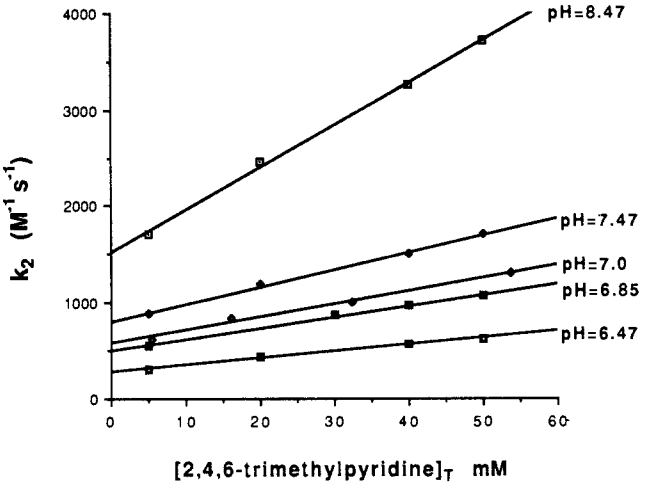

Figure 5. Dependence of the apparent second-order rate constant (k_2') on the concentration of total 2,4,6-trimethylpyridine buffer at various pH values. The values of k_2' that were used in this figure were obtained from plots of k_{obsd} vs [(**2**)$Fe^{III}(H_2O)(X)$] as is shown in Figure 4.

third-order rate constant k_{BT} can be expressed in terms of rate constants for buffer acid (k_{ba}) and buffer base (k_{bb}) catalysis of the reaction of the species (**2**)$Fe^{III}(OH)(H_2O)$ with H_2O_2 (eq 4, where K_a and K_b = the acid dissociation constants of (**2**)$Fe^{III}(H_2O)_2$ and 2,4,6-trimethylpyridine·H^+, respectively). A plot of

$$k_{BT} = \left(\frac{k_{bb}K_b}{(K_b + a_H)} + \frac{k_{ba}(a_H)}{(K_b + a_H)} \right) \frac{K_a}{(K_a + a_H)} \qquad (4)$$

$k_{BT}[(K_a + a_H)/K_a](K_b + a_H)$ vs a_H gives k_{ba} as the slope and $k_{bb}K_b$ as the intercept. From Figure 6 we obtain k_{ba} = 2.5 × 10^5 M^{-2} s^{-1}, and the value for k_{bb} was found to be zero. Similar treatment for 2,6-dimethylpyridine buffers provides k_{ba} = 1.10 × 10^6 M^{-2} s^{-1}, while for 4-methoxy-2,6-dimethylpyridine k_{ba} = 8.99 × 10^4 M^{-2} s^{-1}.

Influence of pyridine *N*-oxide on the rate of reaction of (2)-$Fe^{III}(H_2O)(X)$ with hydrogen peroxide was investigated at concentrations of iron(III) porphyrin of 5 × 10^{-7} and 5 × 10^{-6} M and initial concentrations of hydrogen peroxide and ABTS at 5 × 10^{-5} and 7 × 10^{-3} M, respectively. There was seen to be no evidence for ligation of pyridine *N*-oxide to (**2**)$Fe^{III}(H_2O)(X)$ at pH 6.6. Values of k_{obsd} were found to be the same, within experimental error, in the presence of [pyridine *N*-oxide] = 2 × 10^{-4} M and in the absence of pyridine *N*-oxide. The concentration of the better ligating pyridine *N*-oxide exceeds, in these experiments, the concentration of any 2,6-dimethylpyridine *N*-oxide that could be formed in the reaction of hydrogen peroxide with the iron(III) porphyrin by 100-fold. Thus, any assumption that the kinetic effects of the substituted 2,6-dimethylpyridine·H^+/2,6-dimethylpyridine buffers is due to N-oxidation followed by N-oxide ligation to (**2**)$Fe^{III}(H_2O)(X)$ may be dismissed.

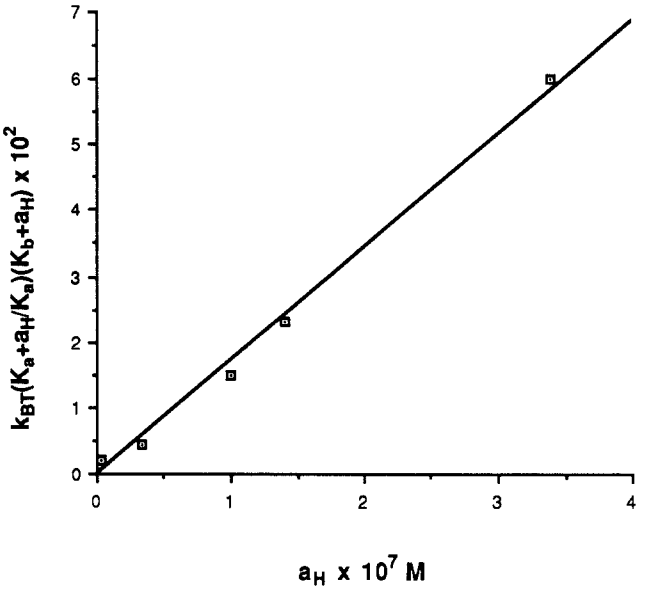

Figure 6. Plot of $k_{BT}[(K_a + a_H)/K_a](K_b + a_H)$ vs a_H. The slope gives k_{ba}, while the intercept gives $k_{bb}K_b$. The values of k_{BT} were obtained from the slopes of the lines in Figure 5.

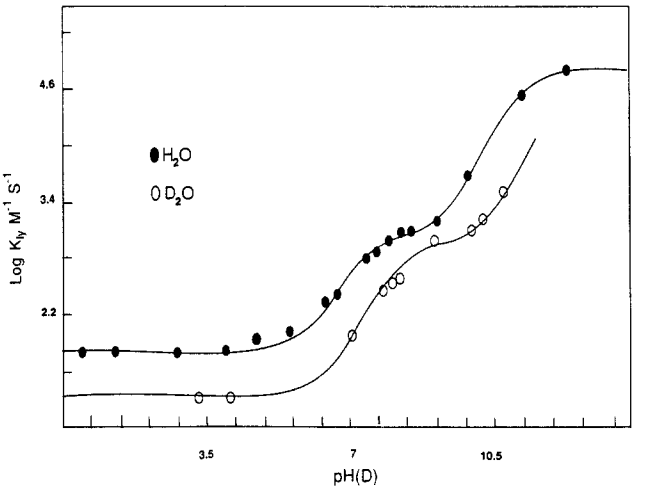

Figure 7. The pH and pD dependence of the log of the nonbuffer-catalyzed rate constants (k_{ly}) for the reaction of (**2**)$Fe^{III}(H_2O)(X)$ with H_2O_2 in H_2O (closed circles) and D_2O (open circles), respectively.

Dependence of k_{ly} upon pH for the Reaction of (2)$Fe^{III}(H_2O)(X)$ with Hydrogen Peroxide. Values of k_{ly} were determined in the pH range 0.5–12.25. For the pH values of 0.5 and 1.3 buffering was with HCl (H_3O^+/H_2O). At the higher pH values of 11.20 and 12.25, KOH solutions were employed (H_2O/HO^- buffer). Buffers used at intermediate pH have been identified (loc. cit.). For pH values less than 4, the experiments were carried out under an O_2 free N_2 atmosphere to avoid an O_2 dependent zero-order appearance of $ABTS^{\bullet+}$.

A plot of log k_{ly} vs pH is shown in Figure 7 where the experimental points have been computer fit to eq 5 (standard error of 5 × 10^{-2}). The values of the derived constants are given in Table II.

$$k_{ly} = \frac{k_a a_H}{(K_A + a_H)} + \frac{k_b K_A}{(K_A + a_H)} + \frac{k_c K_A K_B}{(K_A + a_H)(K_B + a_H)} \qquad (5)$$

Solvent Kinetic Deuterium Isotope Effects. The reaction of the iron(III) porphyrin with hydrogen peroxide was studied over the pD range of 3.3–10.7. Correction for the glass-electrode to read pD was made by the addition of the constant 0.38 (correction at 30 °C)[6] to the pH meter reading. The buffers used were as follows: $ClCH_2CO_2D/ClCH_2CO_2^-$ (0.05 M, pD 3.3 and 4.16),

Table II. Values of Rate and Equilibrium Constants Obtained from the Fitting of Eq 5 to the Experimental Values of k_{ly} Obtained in H_2O and D_2O (Figure 7)

solvent, H_2O				solvent, D_2O			
k_a	67			k_a	22		
k_b	1.08×10^3			k_b	900		
k_c	6.19×10^4						
K_A	5.25×10^{-8}	pK_A	7.28	K_A	7.6×10^{-9}	pK_A	8.12
K_B	7.90×10^{-12}	pK_B	11.10				

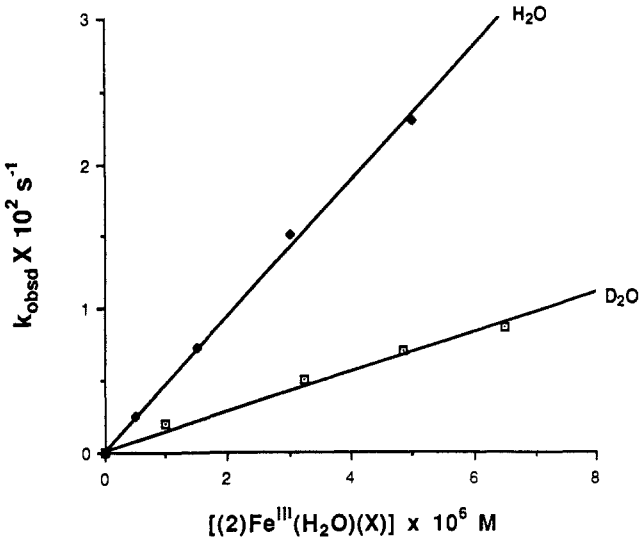

Figure 8. Observed first-order-rate constants at pH = pD = 9.95 (0.05 M carbonate buffer, 30 °C and μ = 0.2) for the formation of $ABTS^{\bullet+}$ as a function of $[(2)Fe^{III}(H_2O)(X)]$. The initial concentrations of H_2O_2 and ABTS were 5×10^{-5} and 7×10^{-3} M, respectively.

2,4,6-trimethylpyridine·D^+/2,4,6-trimethylpyridine (5–50 mM, pD 7.07, 7.80, 8.05, and 9.05), $D_2PO_4^-/DPO_4^{2-}$ (pD 8.39), and DCO_3^{2-}/CO_3^{3-} (pD 9.95 and 10.25 and 10.70). The kinetic runs in D_2O were carried out under the same conditions as those in H_2O, where $[(2)Fe^{III}(D_2O)(X)] < [D_2O_2] \ll [ABTS]$ at 30 °C and ionic strength of 0.2. The buffer-independent second-order rate constants in D_2O (k_{ly}^D) were obtained either from the slopes of plots of k_{obsd} vs $[(2)Fe^{III}(D_2O)(X)]$ or from experiments at a single porphyrin concentration from plots of k_{obsd} vs buffer concentration where k_{ly}^D equals the intercept at zero buffer.

In Figure 8 there is shown an example of plots of k_{obsd} (determined in both H_2O and D_2O) vs iron(III) porphyrin concentration at pH = pD = 9.95. Since there is no buffer catalysis, the values of k_{ly}^H and k_{ly}^D are obtained from the slopes. At this pH(pD) we obtain $k_{ly}^H/k_{ly}^D = 4.52$. In Figure 9 values of $k_2'^D$ are plotted vs the concentration of 2,4,6-trimethylpyridine buffer at a series of pD values. The intercepts represent k_{ly}^D, and the slopes equal k_{BT}^D. As in the experiments in water, from eq 4 a plot of $k_{BT}^D[(K_a^D + a_D)/K_a^D](K_b^D + a_D)$ vs a_D (Figure 10) provides as slope k_{ba}^D (1.20×10^5 M^{-2} s^{-1}) and zero intercept. The value of $k_{ba}^H/k_{ba}^D = 2$.

Values of log k_{ly}^D determined at various fixed pD were fitted to eq 5, and the plot of log k_{ly}^D vs pD is included in Figure 7. It is seen that the experimental points obtained in D_2O fit the log rate constant vs pD profile well (standard error = 8×10^{-2}). The values of the constants employed in the fitting of experimental points to eq 5 are included in Table II. It is evident that the kinetic deuterium isotope effects given by k_{ly}^H/k_{ly}^D at pH = pD is dependent upon the activity of H_3O^+ (D_3O^+). At low pH(pD) $k_{ly}^H/k_{ly}^D = 3$ and from pH(pD) 7–10.7 k_{ly}^H/k_{ly}^D varies from 5.5 to 1.36 back to 4.5 with the smallest value occurring at pH(pD) 9.10. Deuterium solvent kinetic isotope effects could not be determined above pH(pD) = 10.7 since the yields of $ABTS^{\bullet+}$ in reactions carried out in D_2O at high pD are 50% less than for reactions carried out in H_2O at high pH. This decrease in $ABTS^{\bullet+}$ yield in D_2O does not allow an accurate determination of k_{obsd}

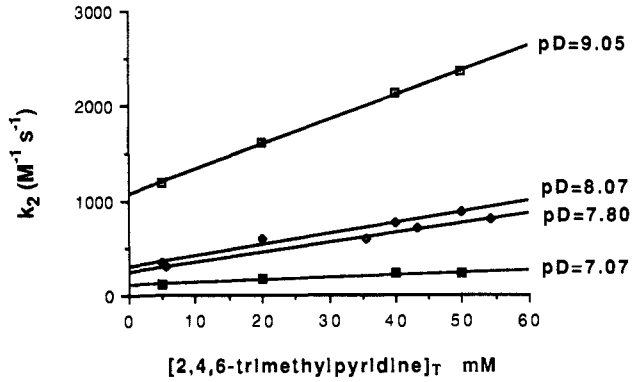

Figure 9. Dependence of the apparent second-order rate constant ($k_2'^D$) for the reaction of $(2)Fe^{III}(H_2O)(X)$ with H_2O_2 on the concentration of total 2,4,6-trimethylpyridine buffer at various pD values.

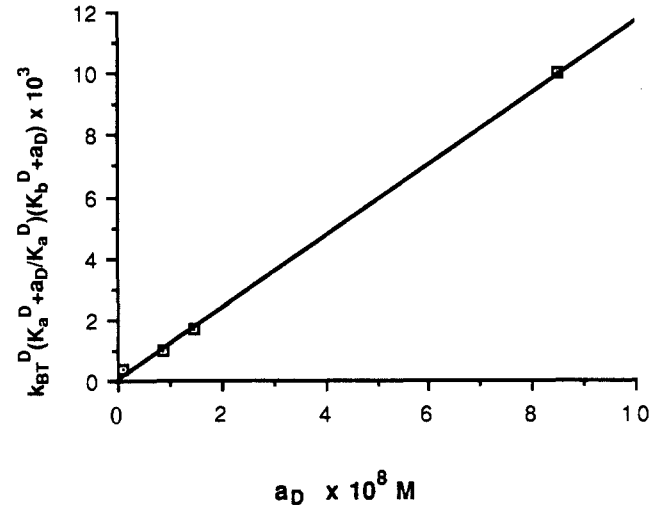

Figure 10. Plot of $k_{BT}^D[(K_a^D + a_D)/K_a^D](K_b^D + a_D)$ vs a_D. The slope gives k_{ba}^D, while the intercept gives $k_{bb}^D K_b^D$. The values of k_{BT}^D were obtained from the slopes of the lines in Figure 9.

values. Since the yield of $ABTS^{\bullet+}$ at high pD in D_2O is less than that at high pH in H_2O, there is a decided kinetic solvent isotope effect on the reaction of hydroperoxide anion (k_{HOO^-}) with hypervalent iron-oxo porphyrin such that $k_{DOO^-}/k_{HOO^-} > 1$.

Discussion

The dynamics of reaction of hydrogen peroxide with the non μ-oxo dimer forming 5,10,15,20-tetrakis(2,6-dichloro-3-sulfonatophenyl)porphinatoiron(III) hydrate $[(2)Fe^{III}(Y_2O)(X)]$; in H_2O, Y = H and X = H_2O or ^-OH, in D_2O, Y = D and X = D_2O or ^-OD] has been investigated in buffered H_2O and D_2O solutions between pH 0.5 and 12.25 and pD 3.3 and 10.70 (30 °C and μ = 0.2 with $NaNO_3$). In order to determine the pH-dependent second-order rate constants (k_{ly}), ABTS was employed as a trap for oxidizing species formed in the rate-determining step. Reactions were first-order in $(2)Fe^{III}(Y_2O)(X)$ and H_2O_2 and zero-order in ABTS.

The pK_a values of H_2O or D_2O ligated to $(2)Fe^{III}(Y_2O)_2$ (Y = H or D) were found to be 7.85 ± 0.1 and 8.68 ± 0.15, respectively. This represents an isotope effect of $K_a^H/K_a^D = 6.76$. Though the pK_a of H_2O is decreased by 7.9 pK_a units on ligation to the Fe(III) moiety, the value of K_a^H/K_a^D compares favorably to the isotope effect on the autoprotolysis constant of water ($K_w^H/K_w^D = 6.5$).[9] The pK_a of 5,10,15,20-tetrakis(2,6-dimethyl-3-sulfonatophenyl)porphyrinatoiron(III) hydrate ($(1)Fe^{III}(H_2O)_2$) has previously been shown to be 7.25[1n] making it a stronger acid than $(2)Fe^{III}(H_2O)_2$. Considering inductive effects alone, the pK_a values

(9) Bunton, C. A.; Shiner, V. J. *J. Am. Chem. Soc.* **1961**, *83*, 42.

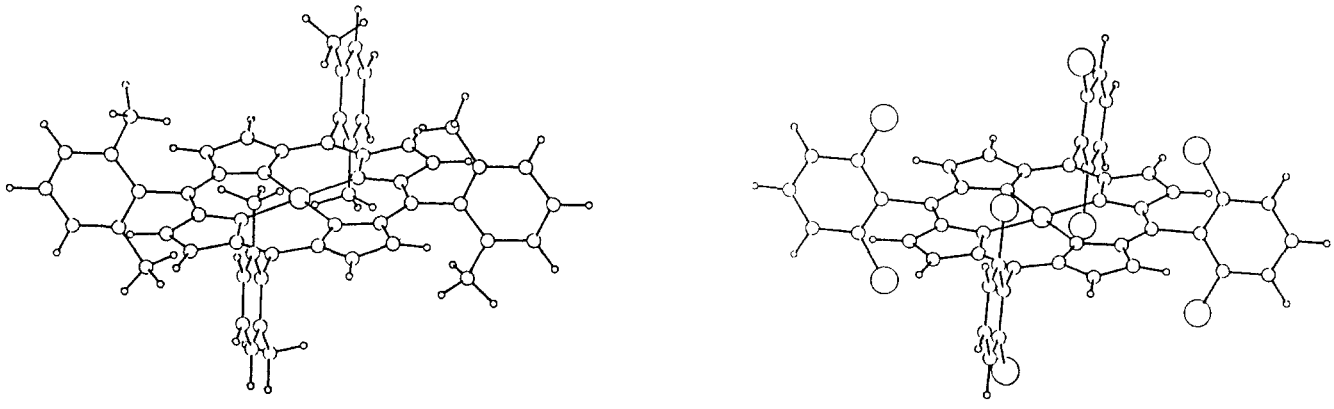

Figure 11. [5,10,15,20-Tetrakis(2,6-dimethylphenyl)porphinatoiron(III)]$^+$ (left) and [5,10,15,20-tetrakis(2,6-dichlorophenyl)porphinatoiron(III)]$^+$ (right). The structures have been generated from an X-ray structure of [5,10,15,20-tetrakis(phenyl)porphinatoiron(III)] chloride by computer substituted of Me- and Cl- for H-atoms at the ortho positions of the phenyl rings and energy minimization of the phenyl–porphyrin bond angle. Axial ligand not shown.

Scheme I

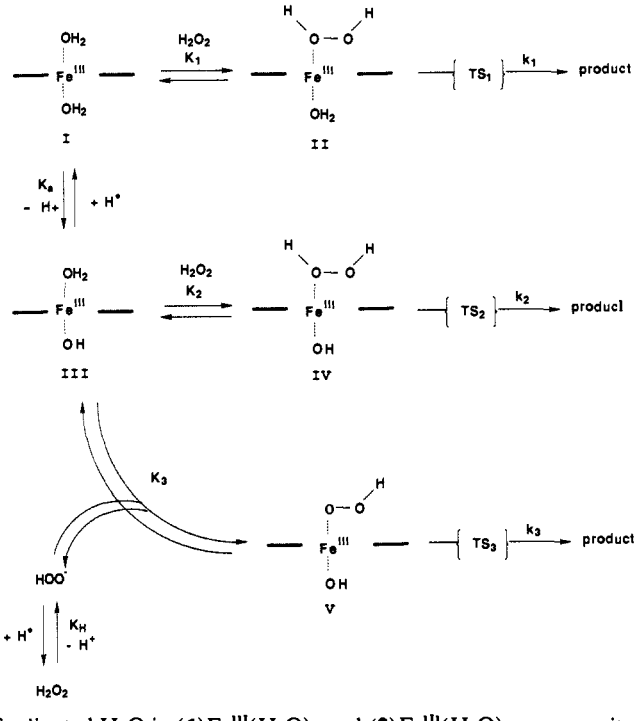

for ligated H_2O in (**1**)$Fe^{III}(H_2O)_2$ and (**2**)$Fe^{III}(H_2O)_2$ are opposite of what is expected. This may be due to a field effect. In (**1**)-$Fe^{III}(H_2O)_2$ four methyl substituents point into the cavity where the ligated H_2O resides, whereas in (**2**)$Fe^{III}(H_2O)_2$ it is four chloro substituents which point toward the ligated water (Figure 11). The influence of such field effects on acidity is very well documented.[10]

The dependence of k_{ly} on pH for oxidative oxygen transfer from hydrogen peroxide to (2)$Fe^{III}(H_2O)(X)$ is discussed in terms of the reaction sequence of Scheme I. The empirical eq 5, used to fit the experimental points in Figure 7, is mathematically equivalent to eq 6a which may be derived from Scheme I with the assumption of preequilibrium complexation of hydrogen peroxide by metalloporphyrin. The three different reaction paths

$$k_{ly} = \frac{k_1K_1a_{H^2} + k_2K_2K_a a_H + k_3K_3K_aK_H}{K_HK_a + (K_H + K_a)a_H + a_{H^2}} \qquad (6a)$$

of Scheme I are seen as three pH independent values of log k_{ly} in Figure 7. The transition states for the three reaction paths differ in the number of protons that are involved. The reacting species at low pH are (**2**)$Fe^{III}(H_2O)_2$ and H_2O_2, at intermediate pH they are (**2**)$Fe^{III}(H_2O)(OH)$ and H_2O_2, and at high pH they are (**2**)$Fe^{III}(H_2O)(OH)$ and HOO^-. In eq 6a, $a_H > K_a \gg K_H$ at low pH, and eq 6a reduces to eq 6b. At intermediate pH, $K_a > a_H > K_H$, and eq 6a reduces to eq 6c. At high pH, $K_a \gg K_H \gg a_H$, and eq 6a reduces to eq 6d. Therefore, k_{ly} can be expressed as a summation of eqs 6b, 6c, and 6d (eq 7). Comparison of the

$$k_{ly} = k_1K_1a_H/(K_a + a_H) = k_{(A)} \qquad (6b)$$

$$k_{ly} = k_2K_2K_a/(K_a + a_H) = k_{(B)} \qquad (6c)$$

$$k_{ly} = k_3K_3K_HK_a/(K_a + a_H)(K_H + a_H) = k_{(C)} \qquad (6d)$$

$$k_{ly} = k_{(A)} + k_{(B)} + k_{(C)} \qquad (7)$$

empirical eq 5, used to fit the pH vs log k_{ly} profile, to eq 7 provides the following equalities: $k_a = k_1K_1$, $k_b = k_2K_2$, $k_c = k_3K_3$, $K_A = K_a$, and $K_B = K_H$. (Experimentally determined values of k_a, k_b, k_c, K_A, and K_B are provided in Table II.) The rate constants k_1, k_2, and k_3 cannot be independently determined due to the composite nature of the derived expressions. The kinetically derived acid dissociation constants ($pK_A = 7.28$ and $pK_B = 11.10$) deviate from the thermodynamically determined acid dissociation constants of (**2**)$Fe^{III}(H_2O)_2$ ($pK_a = 7.85$) and H_2O_2 ($pK_H = 11.6$).[11] Deviations of kinetic apparent pK_a values from the thermodynamic pK_a constant by 0.5 are not unusual and can be caused by any additional preequilibrium step with K_{eq} of ~2–9.[12]

Two arguments may be presented to explain the increase in k_{ly} with an increase in pH: (a) the increase in k_{ly} is a result of more favorable complexation of H_2O_2 to the iron(III) porphyrin as the pH increases or (b) the increase in k_{ly} reflects increasing rates of O–O bond scission with increasing pH. Complexation of H_2O_2 to (**2**)$Fe^{III}(H_2O)_2$ should be more favorable than is complexation of H_2O_2 to (**2**)$Fe^{III}(H_2O)(OH)$ because the former species has a formal positive charge and the latter is neutral. Additionally, K_3 involves the ligation of two anions as axial ligands to an iron(III) porphyrin species. Such species are known in aprotic solvents[13] but are not common. Therefore, it is reasonable to suspect that $K_1 > K_2 > K_3$. Thus, the increase in k_{ly} with increase in pH reflects the increase in the rate of the commitment step for O–O bond scission.

The Effect of Changing the Solvent from H_2O to D_2O and the Influence of Buffer Concentration on the Kinetics of Reaction of Hydrogen Peroxide with the Iron(III) Porphyrin at Low and Intermediate pH Values. The deuterium solvent isotope effects on

(10) (a) Reynolds, W. F. *J. Chem. Soc., Perkin Trans. II* **1980**, 985. (b) Stock, L. M. *J. Chem. Educ.* **1972**, *49*, 400. (c) Topsom, R. D. *Prog. Phys. Org. Chem.* **1976**, *12*, 1. (D) Rees, J. M.; Ridd, J. H.; Ricci, A. *J. Chem. Soc., Perkin Trans. II* **1976**, 224. (e) Acevedo, S.; Bowden, K. *J. Chem. Soc., Chem. Commun.* **1977**, 608. (f) March, J. *Advanced Organic Chemistry*, 3rd ed.; Wiley-Interscience: New York, 1985; p 16.

(11) Kelly, H. C.; Davies, D. M.; King, M. J.; Jones, P. *Biochemistry* **1971**, *16*, 3974.

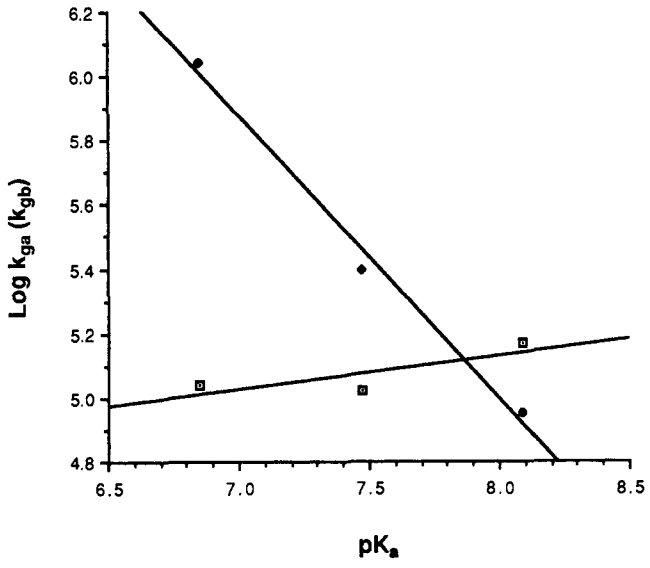

Figure 12. Bronsted plots of the log of the rate constants for general-acid (k_{ga}, closed symbols) and general-base (k_{gb}, open symbols) catalysis in the kinetically equivalent reactions of substituted 2,6-dimethylpyridine·H^+ with (**2**)$Fe^{III}(HO^-)(H_2O_2)$ and substituted 2,6-dimethylpyridine with (**2**)$Fe^{III}(H_2O)(H_2O_2)$ vs the pK_a of substituted 2.6-dimethylpyridine·H^+ species.

k_{ly} are obtained by comparison of the log $k_{ly}{}^H$ and log $k_{ly}{}^D$ vs pH(D) profiles of Figure 7. Experimental values of $k_a{}^D$, $k_b{}^D$, and $K_A{}^D$ are included in Table II. From the kinetic terms of Table II, $k_a{}^H/k_a{}^D = (K_1{}^H/K_1{}^D)(k_1{}^H/k_1{}^D) = 3$, $k_b{}^H/k_b{}^D = (k_2{}^H/k_2{}^D)(K_2{}^H/K_2{}^D) = 1.2$, and $K_A{}^H/K_A{}^D = 6.9$. The isotope effect on the kinetically apparent dissociation constant ($K_A{}^H/K_A{}^D$) compares well with the isotope effect on the thermodynamically derived acid dissociation constant of 6.75. Since ($K_1{}^H/K_1{}^D$) and ($K_2{}^H/K_2{}^D$) are secondary equilibrium isotope effects, they should be equal to or only slightly less than 1.0 such that the kinetic deuterium solvent isotope effects ($k_1{}^H/k_1{}^D$) = ~3 and ($k_2{}^H/k_2{}^D$) = ~1.2. An isotope effect of ~3 supports proton movement in the transition state for O–O bond breaking at low pH (first plateau region of Figure 7), whereas an isotope effect of 1.2 only reflects the transfer of the reaction (pH region of the first ascending and second plateau regions of the log k_{ly} vs pH profile) from H_2O to D_2O.

At the lower plateau, the reaction is not subject to specific-acid or general-acid catalysis. Thus, at low pH values, k_{ly} does not increase with an increase in [H_3O^+] or [$ClCH_2CO_2H$] or [CH_3CO_2H].

At pH values in the first ascending and second plateau regions of the log k_{ly} vs pH profile, catalysis is not seen when using a series of (oxy acid)/(oxy anion) buffers to a concentration of 0.05 M. Catalysis is, however, observed when using substituted 2,6-dimethylpyridine·H^+/2,6-dimethylpyridine (=BH^+/B:) buffers. The experimentally determined rate law is given in eq 8. Since one

$$\text{rate of buffer-catalyzed reaction} = k_{ba}[(\mathbf{2})Fe^{III}(H_2O)(OH)][H_2O_2][BH^+] \quad (8)$$

cannot identify the position of a proton by kinetic means, there are two kinetic equivalents to eq 8. The three kinetically equivalent structures which may enter the transition state are **i**, **ii**, and **iii**.

$$\underset{\mathbf{i}}{[(\mathbf{2})Fe^{III}(HO^-)(H_2O_2)]\cdot[BH^+]}$$

$$\underset{\mathbf{ii}}{[(\mathbf{2})Fe^{III}(H_2O)(HO_2^-)]\cdot[BH^+]}$$

$$\underset{\mathbf{iii}}{[(\mathbf{2})Fe^{III}(H_2O)(H_2O_2)]\cdot[B:]}$$

The compositions **i** and **ii** represent BH^+ catalysis of the reaction of (**2**)$Fe^{III}(HO^-)(H_2O_2)$ and (**2**)$Fe^{III}(H_2O)(HO_2^-)$, respectively. The composition **iii** represents B: catalysis of the reaction of (**2**)$Fe^{III}(H_2O)(H_2O_2)$. The experimentally determined values of k_{ba} (eq 8) pertain to **i** and **ii**. Since k_{ba} would represent a general acid rate constant, the more familiar term k_{ga} is now employed. The rate constant (k_{gb}) for the kinetically equivalent structure **iii** is $k_{gb} = k_{ga}(K_a/K_b)$ (see eq 9, where K_a is the acid dissociation constant for ligated H_2O and K_b the acid dissociation constant for BH^+). With 2,4,6-trimethylpyridine, the experimentally

$$v = k_{ga}[(\mathbf{2})Fe^{III}(HO^-)(H_2O_2)][BH^+]$$

$$v = (k_{ga}K_a)/K_b[(\mathbf{2})Fe^{III}(H_2O)(H_2O_2)][B] \quad (9)$$

determined value of $k_{ga} = 2.5 \times 10^5\ M^{-2}\ s^{-1}$ and the calculated value of $k_{gb} = 1.07 \times 10^5\ M^{-2}\ s^{-1}$. Either term is kinetically competent. Though the BH^+/B: buffers employed number only three, Bronsted plots of log k_{ga} and log k_{gb} vs pK_a of BH^+ species (Figure 12) provide as slopes $-\alpha = 0.9$ for k_{ga} and $\beta = 0.1$ for k_{gb}.

The solvent kinetic isotope effect for ($k_{ga}{}^H/k_{ga}{}^D$) = 2.0 (Results). From eq 9 there follows eq 10. From the thermodynamic acidities,

$$(k_{gb}{}^H/k_{gb}{}^D) = (k_{ga}{}^H/k_{ga}{}^D)(K_a{}^H/K_a{}^D)(K_b{}^D/K_b{}^H) \quad (10)$$

the value of ($K_a{}^H/K_a{}^D$) = 6.75 and ($K_b{}^D/K_b{}^H$) = 0.25 (this study, loc. cit.), so that ($k_{gb}{}^H/k_{gb}{}^D$) = 3.3. A choice between general-acid catalysis by 2,6-dimethylpyridine·H^+ species and general-base catalysis by 2,6-dimethylpyridines may be made by comparison of solvent kinetic isotope effects on k_{ly}. If general acid catalysis is operative, it would be important in the pH range of the first ascending and second plateau regions of the pH vs log k_{ly} profile. Here the kinetic solvent isotope effect [($k_2{}^H/k_2{}^D$) = 1.2] is quite different than ($k_{ga}{}^H/k_{ga}{}^D$) = 2.0. At the plateau at acid pH, the kinetic solvent isotope effect [($k_1{}^H/k_1{}^D$) = 3.0] is in accord with ($k_{gb}{}^H/k_{gb}{}^D$) = 3.3. We conclude that the substituted 2,6-dimethylpyridine bases are the catalytic species and that the transition state has the composition of **iii**.

Deuterium Solvent Isotope Effect at High pH. Due to complexities (Results), the reaction of hydrogen peroxide with the iron(III) porphyrin could not be determined at the highest values of pD. The composition of the transition state is as shown in Scheme I. The large solvent deuterium isotope effect (Figure 7) may be accounted for by an equilibrium deuterium isotope effect ($K_H{}^H/K_H{}^D = 3.8$) on the ionization of H_2O_2. A deuterium kinetic isotope effect is unlikely because ligated species are HO^- and HOO^-.

Mechanisms for Oxidative Oxygen Transfer. Linear free energy plots of log k_{ly} vs pK_a of YOH, for the reaction of percarboxylic acids, alkyl hydroperoxides, and hydrogen peroxide (YOOH species) with (**1**)$Fe^{III}(H_2O)_2$ at pH 2.2 and 6.7, are supportive of a homolytic O–O bond scission being rate-determining when YOOH represents hydroperoxides.[1a-c,e] In the pH range 0.5–5.0, hydrogen peroxide oxidation of the iron(III) porphyrin involves the decomposition of **iv**. Two characteristics of the reaction are

$$\underset{\mathbf{iv}}{(\mathbf{2})Fe^{III}(H_2O)(H_2O_2)}$$

a complete lack of either specific or general acid catalysis and a kinetic solvent deuterium isotope effect of 3 (i.e., $k_1{}^H/k_1{}^D$ of Scheme I). These observations may be accounted for by preassociation of solvent H_2O with **iv** and partial proton transfer to hydrogen-bonded H_2O in the transition state (Scheme II). Lack of observable general catalysis by RCO_2^- species may be due to a small β for oxygen bases, [H_2O] ≫ [RCO_2^-], the energy for desolvation of an oxy-anion base,[14] and electrostatic repulsion in the transition state.[15] The latter should disfavor the mechanism of Scheme III in comparison to Scheme II. In the mechanism

(12) (a) Bruice, T. C.; Schmir, G. L. *J. Am. Chem. Soc.* **1959**, *81*, 4552. (b) Bruice, T. C.; Benkovic, S. J. *Bioorganic Mechanisms*; W. A. Benjamin: New York, 1966; Vol 1, p 13.

(13) (a) Del Gaudio, J.; La Mar, G. N. *J. Am. Chem. Soc.* **1976**, *98*, 3014. (b) La Mar, G. N.; Del Gaudio, *J. Adv. Chem. Ser.* **1977**, *162*, 207.

(14) (a) Hupe, D. J.; Wu, D. J. *J. Am. Chem. Soc.* **1977**, *99*, 7653. (b) Jencks, W. P.; Brant, S. R.; Gandler, J. R.; Fendrich, G.; Nakamura, C. *J. Am. Chem. Soc.* **1982**, *114*, 7145.

Scheme II

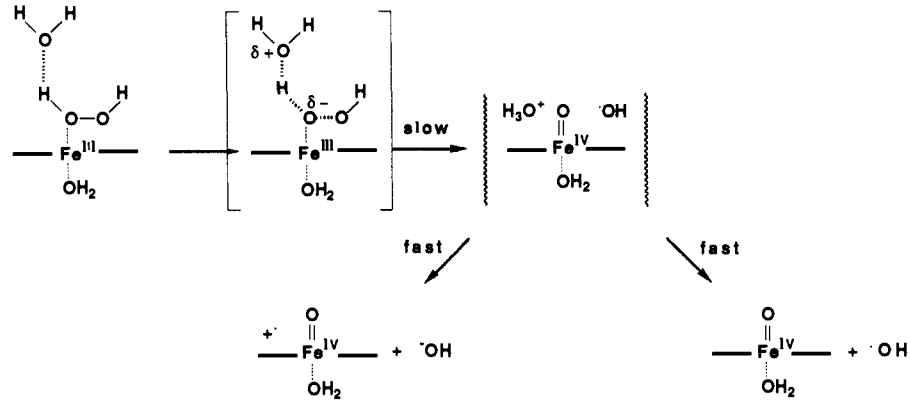

Scheme III

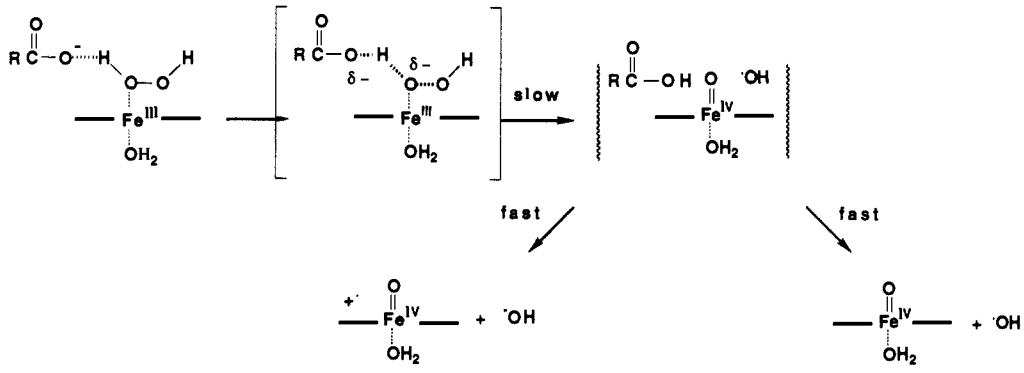

of Scheme II, O–O bond breaking is homolytic to provide solvent caged/iron(IV)-oxo porphyrin + •OH/ which may then partition to solvent-separated species or undergo $1e^-$ oxidation of iron-(IV)-oxo porphyrin by •OH. The latter reaction is thermodynamically favored (eq 11) in aqueous solution ($\Delta G°$ = about −10 kcal/mol). Since the limit for diffusion from a solvent cage[18] is 10^{11} s^{-1} the two processes of partitioning (Scheme II) can compete.

$$(\mathbf{1})Fe^{IV}(O) \rightarrow (\mathbf{1}^{\bullet+})Fe^{IV}(O) + e^- \ (\sim +1.2 \text{ V (SCE)}^{16} \text{ in } H_2O)$$
$$HO^- \rightarrow HO^\bullet + e^- \ (+1.65 \text{ V (SCE)}^{17} \text{ in } H_2O)$$
$$HO^\bullet + (\mathbf{1})Fe^{IV}(O) \rightarrow (\mathbf{1}^{\bullet+})Fe^{IV}(O) + HO^- \ (\text{emf} = -0.45 \text{ V}) \quad (11)$$

In contrast to RCO_2^-, substituted 2,6-dimethylpyridine bases are catalysts for the decomposition of $(\mathbf{2})Fe^{III}(H_2O)(H_2O_2)$. The value of Bronsted $\beta = 0.1$ cannot be said to be known with great accuracy, since it is dependent on the rate constants for only three base species and over a rather narrow pK_a range. Still, it is probably safe to hold that the reaction is general base catalyzed and the transition state is rather early. Since the deuterium kinetic isotope effects for H_2O and 2,4,6-trimethylpyridine are comparable, the general-base homolytic mechanism proposed for H_2O-(D_2O) catalysis of the decomposition of $(\mathbf{2})Fe^{III}(H_2O)(H_2O_2)$ at low pH (Scheme II) may also apply to general base catalysis of the decomposition of $(\mathbf{2})Fe^{III}(H_2O)(H_2O_2)$ by 2,6-dimethylpyridines (where B: replaces H_2O as the base in Scheme II). However, deuterium solvent kinetic isotope effects of 3 for $^1H^+/^2H^+$ transfer from oxygen are not concurrent with a very early transition state. The anticipated isotope effect for an early transition state is dependent upon a knowledge of the value of this isotope effect when the proton has moved half way in the transition state. This is not known for a reaction in which proton movement, electron transfer, and O–O bond breaking are occurring in the transition state.

Chart I

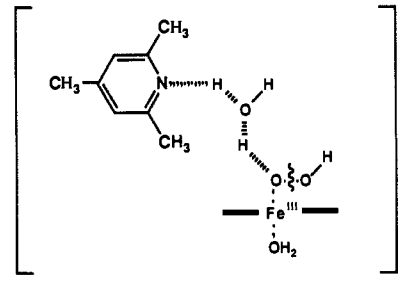

In a Grotthus mechanism where the nitrogen base acts to assist the preassociated water molecule in proton removal (Chart I) the proton transfer to nitrogen could be early and proton transfer to water advanced. For such a mechanism the isotope effect of ~3 would relate to proton transfer to water and β would be small.

In our previous study of the reaction of hydrogen peroxide with $(\mathbf{1})Fe^{III}(H_2O)(X)$ the log k_{ly} vs pH profile closely resembled the profile (Figure 7) of the present study.[1n] Also, as in this study, general catalysis by 2,4,6-trimethylpyridine·H^+/2,4,6-trimethylpyridine buffer was observed. Both the efficiency of substituted 2,6-dimethylpyridines and the small β associated with their catalysis could be explained if these bases were to associate in solution with the tetraphenyl porphyrin moiety. If this were so the mechanism of Scheme II (with B: replacing water) would suffice.

We previously proposed the mechanism of eq 12 for catalysis of the decomposition of $(\mathbf{1})Fe^{III}(H_2O)(H_2O_2)$ by 2,4,6-trimethylpyridine (B:). Catalysis by B: and lack of catalysis by RCO_2^- was attributed to electrostatic stabilization with B: and destabilization with RCO_2^- (eq 13). In eq 12, B: acts as a spectator catalyst so that proton transfer is, to an extent, concerted with O–O bond breaking. For purposes of deliberation, we may look upon the rate of reaction as being dependent on the basicity

(15) (a) Bruice, P. Y. *J. Am. Chem. Soc.* **1984**, *106*, 5959. (b) Ewing, S. P.; Lockshon, D.; Jencks, W. P. *J. Am. Chem. Soc.* **1980**, *102*, 3072. (c) Kresge, A. J.; Chiang, Y. *J. Am. Chem. Soc.* **1973**, *95*, 803. (d) Kresge, A. J.; Chen, H. L.; Chiang, Y.; Murrill, E.; Payne, M. A.; Sagatys, D. S. *J. Am. Chem. Soc.* **1971**, *93*, 413.

(16) Kaaret, T. W.; Bruice, T. C. Unpublished results.

(17) Sawyer, D. T.; Roberts, J. L., Jr. *Acc. Chem. Res.* **1988**, *21*, 469.

(18) For a discussion of the topic, see: Murdoch, J. *J. Am. Chem. Soc.* **1980**, 102, 71. In solvents other than water tabulated limits for diffusion apart range from $\sim 10^5$ to 10^{12} s^{-1}.

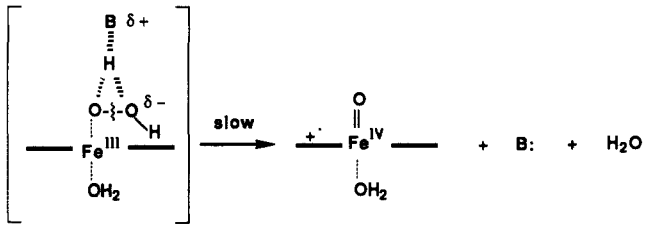

(12)

of B: in proton abstraction and BH^+ in proton donation so that β should be very small. This is as observed. Heterolytic O–O bond scission is expected in eq 12 since the leaving group is H_2O.

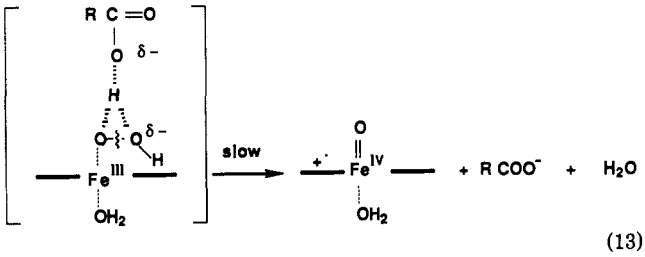

(13)

The complex (**2**)$Fe^{III}(H_2O)(H_2O_2)$ undergoes a H^+ dissociation in the intermediate pH range of 5–9.5 to form either **v** or **vi**. The

$$(\mathbf{2})Fe^{III}(HO^-)(H_2O_2) \qquad (\mathbf{2})Fe^{III}(H_2O)(HO_2^-)$$
$$\mathbf{v} \qquad\qquad \mathbf{vi}$$

rate-determining O–O bond breaking in **v**/**vi** is not associated with a deuterium solvent kinetic isotope effect. General catalysis of the decomposition of **v**/**vi** by (oxy acid)/(oxy base) is not observed. Catalysis by substituted 2,6-dimethylpyridine·H^+ is unlikely (loc. cit.). There is more driving force for O–O bond cleavage in **v** and **vi** as compared to **iii**. This may explain the lack of general catalysis (and isotope effect)—it is not needed.

In order to gain information as to whether the breakdown of **v**/**vi** generates a $(\mathbf{2}^{\bullet+})Fe^{IV}(O)(X)$ species we investigated, in separate experiments, the epoxidation of 3-cyclohexene-1-carboxylic acid at pH 7 with $[(\mathbf{2})Fe^{III}(H_2O)_2]_i = 5 \times 10^{-4}$ M, $[H_2O_2]_i = 0.1$ M, and [alkene] = 1.0 M by using procedures previously[1a] described. Under these conditions there can be 200 turnovers of the iron(III) porphyrin catalyst. Analysis of the reaction mixture showed that a few percent of epoxide was generated; however, this occurred in both the presence and absence of $(\mathbf{2})Fe^{III}(H_2O)_2$. In the course of the experiment 90% of the catalyst was destroyed. Aside from porphyrin destruction, in competition with any plausible epoxidation, there are the reactions of hydrogen peroxide with $(\mathbf{2})Fe^{IV}(O)(X)$ and any $(\mathbf{2}^{\bullet+})Fe^{IV}(O)(X)$ (eqs 14 and 15). The reaction of eq 14 is discussed elsewhere.[1a,b]

$$(\mathbf{2})Fe^{IV}(O)(X) + H_2O_2 \rightarrow (\mathbf{2})Fe^{III}(H_2O)(X) + HOO^{\bullet} + H^+ \quad (14)$$

$$(\mathbf{2}^{\bullet+})Fe^{IV}(O)(X) + H_2O_2 \rightarrow (\mathbf{2})Fe^{III}(H_2O)(X) + O_2 + H_2O \quad (15)$$

Conclusions Concerning the Importance of General Catalysis

The oxidative oxygen transfer reactions which occur after ligation of hydrogen peroxide to 5,10,15,20-tetrakis(2,6-dichloro-3-sulfonatophenyl)porphinatoiron(III) proceed, dependent upon pH, through decomposition of the intermediates $(porph)Fe^{III}(H_2O)(H_2O_2)$, $(porph)Fe^{III}(HO^-)(H_2O_2)$, and $(porph)Fe^{III}(HO^-)(HO_2^-)$. The decomposition of these three species is not subject to general acid catalysis at any pH (H_3O^+, $ClCH_2COOH$, CH_3COOH, $H_2PO_4^-$, and HCO_3^- are not catalysts).

Traylor has concluded that general acid catalysis is diagnostic of heterolytic O–O bond cleavage in the reaction of acyl and alkyl hydroperoxides with iron(III) porphyrins.[19] By this criteria, the reactions of hydrogen peroxide with the iron(III) porphyrin of this study represents O–O bond homolysis. We consider that O–O bond homolysis in the reaction of hydrogen peroxide and alkyl hydroperoxides with iron(III) porphyrins is likely rate-determining. We do not, however, believe that it has been shown that general acid catalysis is diagnostic of heterolytic O–O bond breaking. Quite the contrary, there are no studies in the literature that support this contention notwithstanding the references[20,21] provided by Traylor.[19] Groves has recently established that the decomposition, in an aprotic solvent, of an iron(III) porphyrin ligated by acyl peroxide anion is specific-acid (rather than general-acid) catalyzed.[22] This finding is not unexpected since without protonation the reaction provides RCO_2^-, an unstable leaving group in an aprotic solvent (eq 16).

$$(porph)Fe^{III}(RCO_3^-) + H^+ \rightarrow (porph^{\bullet+})Fe^{IV}(O)(X) + RCO_2H \quad (16)$$

Traylor and co-workers[19,23] as well as ourselves[1e] have studied the reaction of acyl and alkyl hydroperoxides with iron(III) porphyrins in the protic solvent methanol. We recognized the severe limitations of this solvent in the interpretation of results and have changed to the protic solvent water (this and the following paper in this journal as well as ref 1a–d,g,n). Although Traylor favors the importance of general-acid catalysis, he is not able to interpret his data as supporting general-acid over general-base catalysis. [This situation arises because the activity of lyate acid species (H_3O^+ and $CH_3OH_2^+$) in the reaction solutions and the pK_a values of buffer acid and MeOH ligated to iron(III) porphyrin were not determined in MeOH, and, also, the influence on rate of the overlapping acid dissociations of both the buffer-acid species and iron(III) porphyrin ligated MeOH were not accounted for. Thus, the conclusions were based on the increase in rate with total buffer concentration.] Even his second-order rate constants are suspect since some reactions were carried out without buffering, and all reactions are carried out without the maintenance of constant ionic strength. Indeed, in some experiments designed to determine the dependence of rate on a reactant, the ionic strength was varied from ~0 to 0.5.

We find substituted 2,6-dimethylpyridines serve as general base catalysts for decomposition of the species $[(\mathbf{2})Fe^{III}(H_2O)(H_2O_2)]$ which exists below pH 5 where solvent water also acts as a general-base catalyst. Plausible mechanisms have been discussed. General-base catalysis by oxygen bases ($ClCH_2COO^-$, CH_3COO^-, HPO_4^{2-}, CO_3^{2-}, and HO^-) is not observed at any pH.

Acknowledgment. The present study was supported by grants from the NIH and NSF.

(19) Traylor, T. G.; Ciccone, J. P. *J. Am. Chem. Soc.* **1989**, *111*, 8413.
(20) Hideya, F.; Winstein, S. *J. Am. Chem. Soc.* **1967**, *89*, 1661.
(21) Hassel, C. H. *Org. React.* **1957**, *9*, 73.
(22) Groves, J. T.; Watanabe, Y. *J. Am. Chem. Soc.* **1988**, *110*, 8443.
(23) Traylor, T. G.; Lee, W. A.; Stynes, D. V. *J. Am. Chem. Soc.* **1984**, *106*, 755.